HAVSTOVAN
FAROE MARINE RESEARCH INSTITUTE

Monitoring the flow of Atlantic water through the Faroe-Shetland Channel

Tórshavn · December 2013

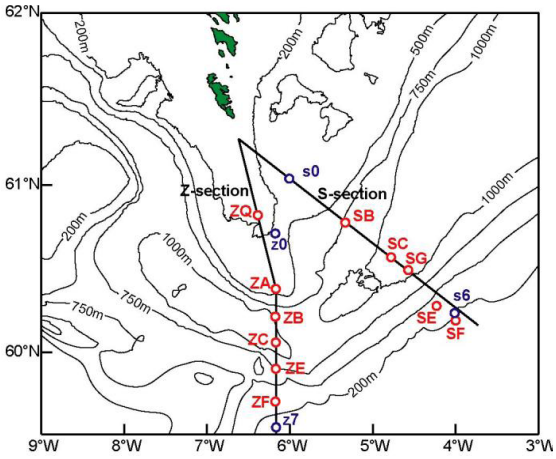

Bogi Hansen, Karin M. H. Larsen

Hjálmar Hátún, Regin Kristiansen

Ebba Mortensen, Barbara Berx

Toby Sherwin, Svein Østerhus

Detlef Quadfasel, Kerstin Jochumsen

HAVSTOVAN NR.: 13-13
TECHNICAL REPORT

Monitoring the flow of Atlantic water through the Faroe-Shetland Channel

Bogi Hansen[1], Karin M. H. Larsen[1], Hjálmar Hátún[1], Regin Kristiansen[1], Ebba Mortensen[1], Barbara Berx[2], Toby Sherwin[3], Svein Østerhus[4], Detlef Quadfasel[5], Kerstin Jochumsen[5]

[1]Faroe Marine Research Institute, Nóatún 1, P.O. Box 3051, FO 110 Tórshavn, Faroe Islands
[2]Marine Scotland Science, Marine Laboratory, P.O. Box 101, Aberdeen, AB11 9DB, UK
[3]Scottish Association for Marine Science, Oban, Argyll, PA37 1QA, UK
[4]Uni Bjerknes Centre, Uni Research and University of Bergen, Norway
[5]Institut für Meereskunde, Universität Hamburg, Bundesstrasse 53, 20146 Hamburg, Germany

Abstract

This report presents results from an experiment, carried out in 2011-2012 within the EU-THOR project to investigate whether future monitoring of the Atlantic water transport through the Faroe-Shetland Channel might be more efficiently achieved on another section than the traditional Munken-Fair Isle section. The new section is less affected by meso-scale activity and narrower, allowing better horizontal resolution of the mooring array, but the experiment revealed that moving to the new section involved other drawbacks. The experiment also confirmed an earlier conjecture that data from satellite altimetry might provide better estimates of transport variations than estimates based on in situ measurements, solely. Previous efforts to determine the average volume transport of Atlantic water through the channel and its variations have been hampered by lack of information on the thickness variations of the Atlantic layer. Re-evaluating the historical data set, we find that the transport estimates are not significantly affected by assuming that the lower boundary of the Atlantic layer is fixed, equal to the average 5°C-isotherm. Based on the conclusions of this report, we recommend that future in situ monitoring in the channel is re-focused.

HAVSTOVAN NR.: 13-13
TECHNICAL REPORT

1. Introduction

The flow of warm and saline water from the Atlantic Ocean, across the Greenland-Scotland Ridge, into the Nordic Seas is an important source of heat and salt to the Arctic region and provides most of the water that, after cooling, returns to feed the North Atlantic Thermohaline Circulation. This "Atlantic inflow" is carried by three branches and the branch through the Faroe-Shetland Channel (FSC) contains the warmest and most saline water.

Since the mid-1990s, efforts have been made to monitor current velocity and transport through the FSC by deploying an array of Acoustic Doppler Current Profilers (ADCPs) on one of the long-term hydrographic standard sections in the channel. This section, which runs between Fair Isle on the Shetland side of the channel to Munken on the Faroe shelf, will here be termed the "S-section" (Figure 1).

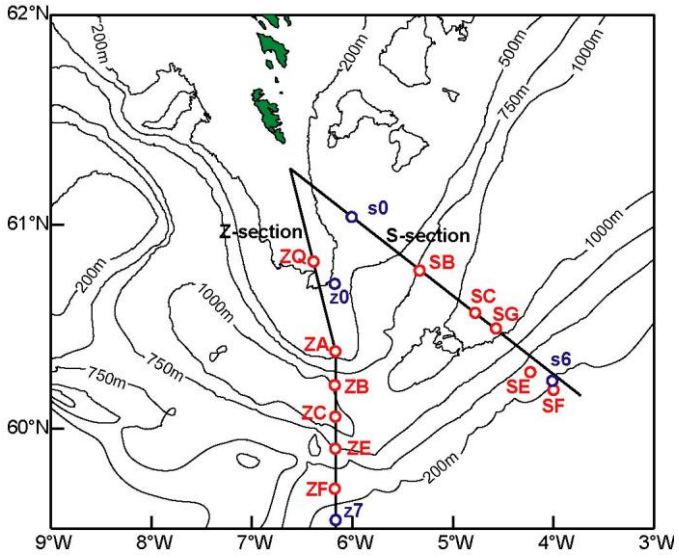

Figure 1. Topographic map of the area with standard sections Z and S shown by black lines, ADCP moorings by red circles, and selected altimetry points by blue circles.

By combining in situ CTD and ADCP measurements from this section with sea level height data from satellite altimetry, it has been possible to estimate the average volume transport of Atlantic water through the FSC and generate a monthly averaged time series of its variation from November 1992 (Berx et al., 2013), but the data clearly show that the conditions on this section are not optimal for in situ transport monitoring due to strong mesoscale activity and recirculation.

In the EU-THOR project (http://www.eu-thor.eu/), it was therefore decided to perform an experiment in which there were parallel ADCP measurements on the S-section and on another section, termed the "Z-section" (Figure 1), which was expected to be less affected by complicating processes. Altogether, six ADCPs were deployed on the Z-section, and five ADCPs on the S-section. The first moorings in this experiment were deployed in May 2011 and the last recoveries were in May 2012. Due to logistical problems, some of the mooring sites were, however, only occupied part of the period and there was no period with full coverage of both sections.

This lack of simultaneous coverage makes it difficult to compare the measurements from the two sections, but it is still possible to draw some conclusions that may help in designing future monitoring systems for the FSC. This is especially important within the EU-NACLIM project (http://www.naclim.eu/), where monitoring of the Atlantic water flow through the FSC is continued.

The first aim of this technical report is to present the main results from this experiment and discuss whether the Z-section is better suited for future in situ monitoring than the S-section, but more

generally, there are various aspects that complicate the monitoring of Atlantic water volume transport through the channel, which need to be addressed.

For the average transport estimate, Berx et al. (2013) combined in situ CTD and ADCP measurements with satellite altimetry to determine the most accurate value. For the temporal transport variations they chose to present a time series based on altimetry, calibrated with in situ measurements, rather than a time series generated from in situ data, solely. This raises the question whether future monitoring should focus on optimizing the in situ measurements so that they can produce transport time series based on these measurements, solely. Or, should the in situ measurements rather aim at better calibration of altimetry-based transport estimates? Or, don't we need further in situ monitoring?

Another problem with the existing data sets is in regard to the coupling between the velocity field and the temperature/salinity fields. Due to heavy fishing activity, traditional moorings with mooring lines extending up into the Atlantic layer cannot be maintained in the channel for prolonged periods. This is the reason that the velocity measurements have been made with ADCPs, moored below the fisheries zone, or deployed in protected zones or in trawl-protected frames on the bottom.

This has, however, had the drawback that the only continuous temperature and salinity measurements are at the ADCPs, mostly below the Atlantic layer. More representative information on the hydrographic fields has had to rely on the snapshot measurements made by CTD cruises. Through a long-term effort, these cruises have provided a sufficient number (~100) of temperature and salinity sections so that reliable average sections can be generated. From these, we know the average properties of the Atlantic layer in the channel and Berx et al. (2013) have shown that the 5°C-isotherm is an appropriate measure of the deeper boundary of the Atlantic layer.

The long-term cruise activity has allowed determination of the average depth of this isotherm at all the standard stations on the S-section and both the average Atlantic water transport and its temporal variation, estimated by Berx et al. (2013), were integrated down to this average isotherm. The 5°C-isotherm depth does, however, vary considerably at each station, but we have not measured these variations with the same temporal resolution as the ADCP data. A priori, we can expect this to affect the time series of transport variations and perhaps even the average transport. To address this question, we have analyzed the CTD and ADCP data from the S-section together with altimetry data.

In addition to presenting the results from the 2011-2012 measurements on the Z-section, this report thus attempts to answer three questions:

- Is the Z-section better suited for in situ transport monitoring than the S-section ?

- Are volume transport variations more accurately monitored by in situ measurements or by satellite altimetry ?

- Does the lower boundary of the Atlantic layer in the channel vary so much that it affects estimates of average transport and its variations ?

2. Material and methods

The main data set is the records from 12 ADCP deployments at 11 mooring sites (Table 1), six of them along the Z-section and the remaining 5 along the S-section (Figure 1). On the Z-section, the mooring sites are denoted ZQ, ZA, ZB, ZC, ZE, and ZF, starting over the Faroe Plateau and moving southwards (Figure 1 and Figure 2). On the S-section, the sites are: SB, SC, SG, SE, and SF, again starting on the Faroe side of the channel.

At ZB and ZC, microcats attached just below the ADCP showed that the moorings were often drawn down considerably, probably due to a strong overflow current. Using the depth readings from the microcats, the bin depths of these ADCPs were adjusted to the reference (no drawdown) depths.

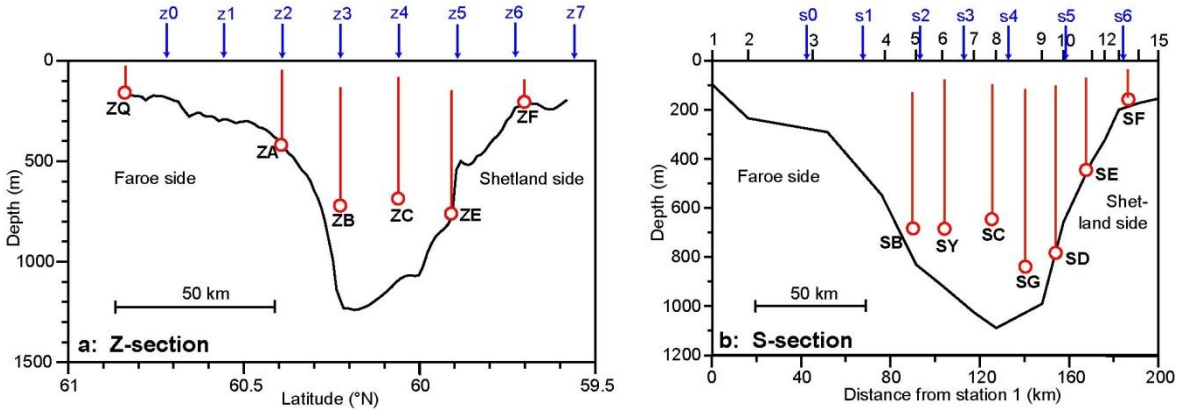

Figure 2. ADCP Deployments along the two sections. Red circles indicate instrument depth (with no draw-down) of ADCPs. Vertical red lines indicate maximum range of the ADCPs (last column in Table 1). The arrows at top, denoted z0 to z7 and s0 to s6 indicate altimetry grid points along the sections. Standard stations 1-15 on the S-section are shown on top in b. Note different horizontal scales in the two panels.

Table 1. Details of the ADCP records, showing location and bottom depth, the period of measurement, the size (thickness) of each bin (Bin), and the (centre) depth of the uppermost bin measured (Top). At site SE, there were two consecutive deployments and the three days from 13. to 15. Dec. 2011 are missing.

Site	Latitude	Longitude	Bottom	Period	Bin	Top
ZQ	60 50.008 N	06 23.553 W	165m	2011.09.05 - 2012.05.18	8m	26m
ZA	60 23.403 N	06 09.590 W	416m	2011.06.12 - 2012.05.17	10m	47m
ZB	60 13.500 N	06 10.000 W	1165m	2011.09.05 - 2012.05.17	10m	140m
ZC	60 04.100 N	06 10.100 W	1080m	2011.09.05 - 2012.05.17	10m	90m
ZE	59 54.360 N	06 10.020 W	775m	2011.12.18 - 2012.05.10	25m	159m
ZF	59 42.300 N	06 09.940 W	208m	2011.10.12 - 2012.05.10	8m	101m
SB	60 47.015 N	05 18.120 W	792m	2011.06.12 - 2012.05.18	10m	76m
SC	60 33.800 N	04 46.300 W	1063m	2011.06.12 - 2012.05.17	25m	84m
SG	60 30.514 N	04 33.997 W	1041m	2011.05.12 - 2011.12.13	25m	100m
SE	60 16.625 N	04 19.860 W	447m	2011.05.11 - 2012.05.14	10m	62m
SF	60 12.000 N	04 00.000 W	168m	2011.05.11 - 2011.10.10	8m	45m

After standard editing and quality control, the series were de-tided and averaged to give daily values and the along-channel velocities calculated for each bin. These are defined to be perpendicular to the sections, i.e. towards 90° for the Z-section and towards 38° for the S-section.

The last column in Table 1 lists the uppermost level measured by each ADCP but, often, the range would be shorter due to low echo or mooring draw-down. It is found, however, that there is generally a tight relationship between along-channel velocities at consecutive bins: $U_j(t) = \alpha_j \cdot U_{j-1}(t)$, where $U_j(t)$ is the along-channel velocity at bin j for the time t. This was checked by correlation

analysis. As shown in Table 2, the correlation coefficients are high, especially for the deep water sites and the regression coefficients (α_j) are all close to one. The regression coefficients were therefore used to extrapolate all the ADCP records to their uppermost bins (last column in Table 1). Above these levels, the along-channel velocity was extrapolated to the surface with the value at the uppermost bin. All the series were then converted to a regular 10m grid centred at 5m, 15m, etc. by linear interpolation between bins. We also use historical CTD and ADCP data from the S-section, the details of which are described by Berx et al. (2013).

Table 2. Relationships between consecutive bins at each site. Column two (Bins) lists the maximum number of bins that may be missing in the top layer for some records (ensembles). This is followed by the range of the correlation coefficient between consecutive bins and the range of the regression coefficient, where the regression is constrained to go through the origin.

Site	Bins	Corr.coeff.	Regr.coeff.(α_j)
ZQ	6	0.864 – 0.992	0.991 – 1.067
ZA	7	0.996 – 0.999	1.006 – 1.016
ZB	6	0.992 – 0.997	1.003 – 1.027
ZC	11	0.992 – 0.998	0.983 – 1.011
ZE	0		
ZF	4	0.962 – 0.985	0.961 – 0.993
SB	8	0.991 – 0.998	0.980 – 1.007
SC	9	0.971 – 0.997	0.936 – 1.052
SG	1	0.986 – 0.998	0.945 – 1.011
SE	4	0.992 – 0.997	0.993 – 1.020
SF	0		

In addition to the in situ data, we also use update MSLA (Mean Sea Level Anomaly) data produced by Ssalto/*Duacs* and distributed by *Aviso*, (http://www.aviso.oceanobs.com/duacs/) with support from *Cnes*. The data are on a rectangular grid with approximately 18 km resolution and are sampled once a week. The Z-section is located almost exactly mid way between two meridional lines of grid points. By averaging these pair-wise, we have generated time series of MSLA values at ten points from z0 at (60.7185°N, 6.1667°W) over the Faroe side to point z9 at (59.2174°N, 6.1667°W) over the Shetland side (Figure 1).

For the S-section, we use the 7 altimetry points, chosen by Berx et al. (2013), from point s0 at (61.0429°N, 6.0000°W) over the Faroe side of the channel to point s6 at (60.2257°N, 4.0000°W) over the Shetland side (Figure 1) and have extended this line south-eastwards to point s9 at (59.7253°N, 3.0000°W).

3. Hydrography and currents on the Z-section

The hydrography on the Z-section is dominated by Atlantic water near the surface and overflow water at depth. An appropriate criterion for Atlantic water is T > 5°C (Berx et al., 2013). On the S-section, the 5°C-isotherm is on average slightly deeper than 500 m over the Shetland side of the channel, ascending to slightly less than 400 m over the Faroe side.

On the Z-section, we do not have a similar set of hydrographic data from standard stations on the section, but the Faroese CTD archive has 199 profiles close to the section of sufficient depth to reach the 5°C-isotherm. A plot of the isotherm depth from these profiles against latitude (Figure 3) indicates an even stronger tilt than for the S-section and the regression line shallows from 633 m at site ZE to 394 m at site ZA. This is consistent with the microcat measurements at ZA, where the overall average (11 months) was 4.81°C with a standard deviation of 1.63°C at a depth of 416 m.

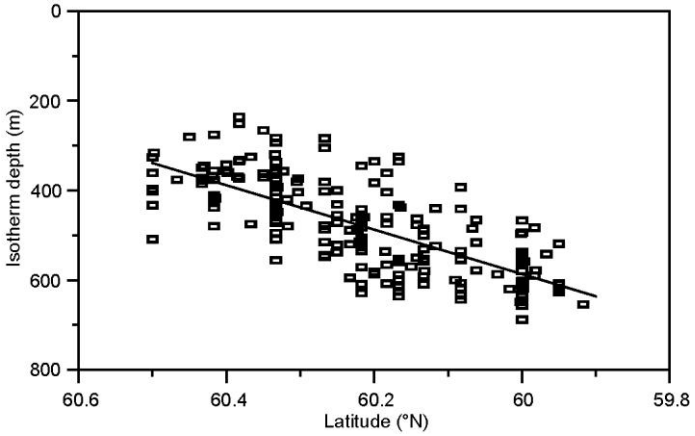

Figure 3. Depth of the 5°C-isotherm on the Z-section, plotted against latitude. Each rectangle is from one CTD profile within an area extending half a degree in longitude east and west from the section. The regression line explains 53% of the variance in isotherm depth.

The thickness of the Atlantic layer varies, but it normally extends at least to 200 m depth all across the section (Figure 3). Figure 4 shows the temporal variation of the (vertically averaged) along-channel velocity of this layer at the various ADCP sites on the Z-section.

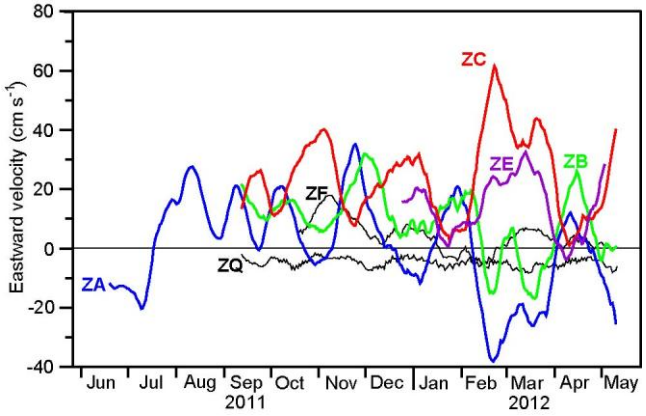

Figure 4. Eastward velocity on the Z-section, averaged from the surface to 200 m or bottom if shallower and averaged over 15 days (running mean).

When considering the deep-water mooring sites (ZA, ZB, ZC, and ZE), the time series in Figure 4 seem to fall into two groups: On the Faroese side, ZA and ZB co-vary and these two series are in anti-phase with ZC and ZE, which also co-vary with one another. Correlation analysis supports this visual impression for 15-day averages and even, to some extent, for 1-day averages (Table 3). The along-channel velocity at site ZQ is weak and relatively stable (Figure 4) and it is not correlated with the velocities at the other sites (Table 3). Probably, it represents the shelf circulation, rather than flow through the channel and it will not be included in the following treatment.

Table 3. Pair-wise correlation coefficients between Atlantic layer (0 – 200 m) eastward velocities from two ADCPs, averaged over 15 non-overlapping days (upper row) and over one day (bottom row). Numbers in brackets indicate the number of values for each correlation analysis.

Averaging	ZQ-ZA	ZA-ZB	ZA-ZC	ZA-ZE	ZB-ZC	ZB-ZE	ZC-ZE
15 days:	0.17(17)	0.91(17)	-0.85(17)	-0.88(9)	-0.80(17)	-0.87(9)	0.85(9)
1 day:	0.03(256)	0.48(256)	-0.66(256)	-0.47(145)	-0.47(256)	-0.47(145)	0.35(145)

In order to present an average velocity section, we have produced average profiles from each of the sites. Unfortunately, all sites on the Z-section were only occupied simultaneously from 18 Dec. 2011

to 10 May 2012. The average section for this period (Figure 5) shows eastward (positive) flow over the southern part of the Z-section. Since this is towards the Norwegian Sea, we term this "inflow". Over the Faroese slope region, there is in this period a counter-flow on the average, which we term an "outflow". From Figure 4, it appears that both the inflow and the outflow may be unusually strong during a large part of this averaging period. Thus, Figure 5 may not necessarily be very representative.

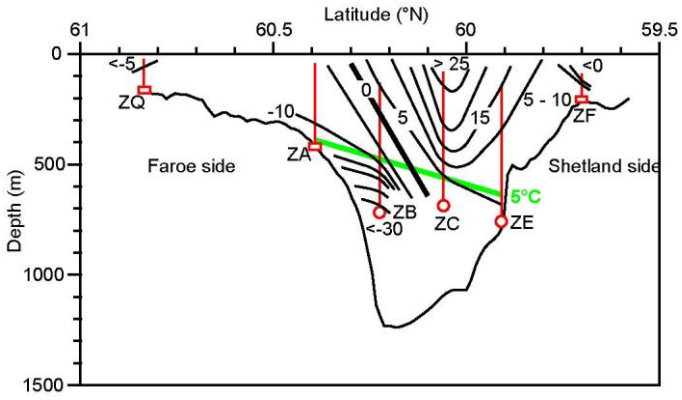

Figure 5. Eastward velocity (cm s^{-1}) on the Z-section, averaged over the period 18. Dec 2011 to 10. May 2012. The thick green line indicates the average 5°C-isotherm as represented by the regression line in Figure 3.

4. Along-channel velocity on the Z-section and altimetry

On weekly time scales, we expect geostrophic balance and weekly averaged surface velocity should therefore be linked to the sea level slope along the section. Since we use MSLA data, absolute values for sea level height are not reliable, but the variations should be. We therefore expect high correlations between variations of the difference in MSLA between two altimetry points and the eastward surface current between the two points. For most of the ADCP sites, that is the case (Table 4).

Table 4. Correlation coefficients between weekly averaged eastward velocities at the ADCP sites on the Z-section and MSLA differences between altimetry grid points. The second row (n) lists number of weeks. The next four rows show correlation and regression coefficients between surface velocity and the average velocity from surface down to the average 5°C-isotherm or bottom. Regression coefficients a and b are from a traditional regression analysis and the offset b is scaled by the rms value of the average velocity. a_0 is when the offset is constrained to zero. Columns 7-9 list correlation coefficients between surface velocity and the MSLA-change across three pairs of altimetry points. Columns 10-12 list correlation coefficients between average velocity and the MSLA-change across three pairs of altimetry points. The pair denoted North extends from the altimetry point close to the site to the next point northwards. The pair denoted South extends from the altimetry point close to the site to the next point southwards. The pair denoted Both extends from the altimetry point north of the site to the point south of it. The highest correlations are underscored.

Site	n	Surf.vel. – Avg.vel.				Surf.vel. – MSLA			Avg.vel. – MSLA		
		Corr.	a	b/rms	a_0	North	South	Both	North	South	Both
ZA	47	0.99	0.79	-0.15	0.78	<u>0.82</u>	0.72	0.79	<u>0.84</u>	0.73	0.80
ZB	35	0.99	0.92	-0.33	0.76	<u>0.57</u>	-0.06	0.46	<u>0.58</u>	-0.07	0.46
ZC	35	0.98	0.86	-0.09	0.80	0.35	<u>0.85</u>	0.76	0.34	<u>0.82</u>	0.74
ZE	19	0.99	0.84	-0.09	0.78	0.66	<u>0.71</u>	0.69	0.70	<u>0.72</u>	0.72
ZF	29	0.97	0.71	0.37	0.78	0.14	<u>0.25</u>	0.19	0.26	<u>0.37</u>	0.31

We also find high correlations between the surface velocity $u_s(t)$ and the velocity averaged from surface down to the 5°C-isotherm $u_a(t)$ (Table 4). This implies that the average velocity is well represented by a linear regression fit: $u_a(t) = a \cdot u_s(t) + b$. For ZA, ZC, and ZE, the offset b is small

compared with the rms value of the average velocity (Table 4), which implies that a modified regression analysis with *b* constrained to zero: $u_a(t) = a_0 \cdot u_s(t)$ should also give a good fit. Generally, Table 4 indicates that the variations in the average velocity are around 80% of the surface velocity variations.

As seen in Figure 2, all of the ADCP sites are close to one of the altimetry points. When comparing MSLA-changes across an altimetry interval and ADCP velocities, we therefore may choose the interval just north of the ADCP site, just south of it, or the combination of both. Table 4 lists correlation coefficients between both surface and average velocities and the MSLA-change across each of these three intervals for each ADCP site. For ZA, ZC, and ZE, we find relatively high correlations, indicating that the link to altimetry explains at least 50% of the variance in both surface and average velocity. For ZB and especially ZF, the correlations are much lower, which may perhaps indicate that the velocities at the ADCP site are not representative for the whole width of any of the altimetry intervals.

5. ADCP-based volume transport through the Z-section

For the period from 18 Dec 2011 to 10 May 2012, all the ADCP sites on the Z-section were instrumented and we can calculate the volume transport of Atlantic water, defined as water warmer than 5°C, through the channel for this period. Over the inner part of the Faroe shelf, there is a closed circulation around the islands (Larsen et al., 2008). To be consistent with previous transport estimates from the S-section, we therefore choose the northern boundary to be at 60.5°N where bottom depth is ~ 300 m. This implies that site ZQ is not used for transport calculation. Similarly, we choose the southern boundary to be at 59.7°N, close to the ZF mooring site. Volume transport will be calculated between these two boundaries, from the surface down to the bottom or the 5°C-isotherm, whichever is shallower. For lack of information, we assume initially that the 5°C-isotherm is fixed and follows the regression line in Figure 3 (green line in Figure 5). In Parts 8 and 9, we discuss isotherm depth variations and their consequences.

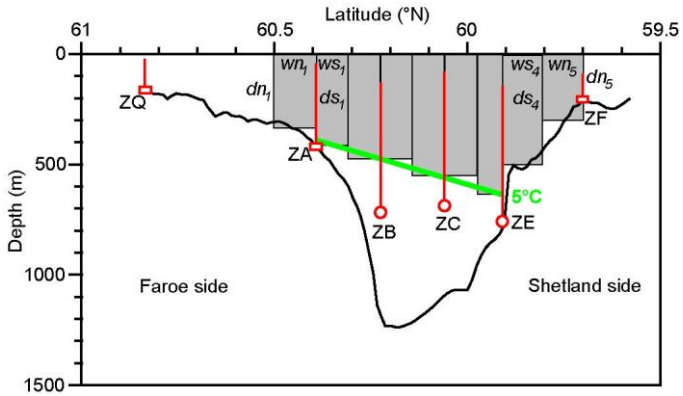

Figure 6. Volume transport of Atlantic water is calculated by adding the transport through nine subareas of the section (grey rectangles) extending northwards or southwards from each of the ADCP sites, except for ZF, which lacks a southern area

Calculation of the volume transport through this cross section involves horizontal inter-polation between the ADCP sites and extrapolation towards the boundaries, which may be done in different ways. We have chosen a simple method, in which the Atlantic water transport *Q(t)* is calculated by adding the transports through nine subareas:

$$Q(t) = \sum_{j=1}^{5} \left[\sum_{i=1}^{dn_j} u_{i,j}(t) \cdot wn_j + \sum_{i=1}^{ds_j} u_{i,j}(t) \cdot ws_j \right] \qquad (1)$$

where the ADCP sites are denoted 1 to 5, going from ZA to ZF, $u_{i,j}(t)$ is the eastward velocity at ADCP site j at depth i and time t. wn_j and ws_j are the widths of the areas associated with site j northwards and southwards of the site, respectively, and dn_j and ds_j are their depths, as illustrated on Figure 6. As we calculate the volume transport only south to ZF, $ws_5 = 0$.

Originally, the intersection between two sites is chosen halfway between them ($wn_{j+1} = ws_j$). Weekly averaged volume transport, calculated in this way, is shown in Figure 7 (red curve) together with the MSLA-change $\Delta z(t)$ between altimetry points z2 close to site ZA and z6 close to site ZF (black curve). The correspondence between these two series is not impressive and the correlation coefficient between them is only 0.54.

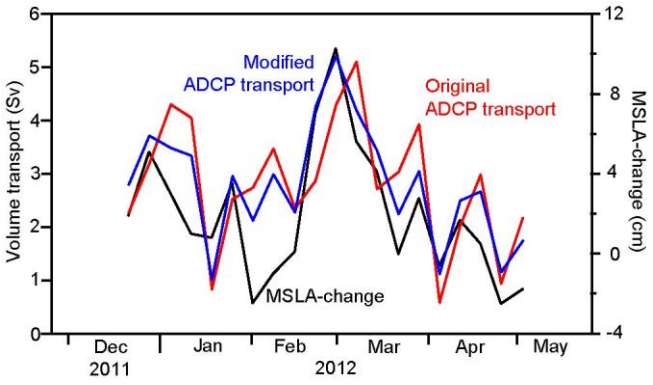

Figure 7. Weekly averaged volume transport through the Z section and MSLA-change across it from 18 Dec 2011 to 10 May 2012. The red curve shows the volume transport calculated from the ADCP velocities assuming the area associated with each ADCP to extend halfway over to the next ADCP. The blue curve shows the volume transport based on the ADCPs with the areas modified to fit better with the altimetry. The black curve shows the MSLA-change between altimetry points z2 and z6 (z6 – z2).

This correlation coefficient is low compared with most of the correlations between individual ADCP velocities and altimetry (Table 4) and the question arises whether this is due to inaccuracies in the link between altimetry and volume transport or uncertainties in our transport estimate.

One problem with the transport estimate is the ad hoc association of areas with each ADCP. To test for the sensitivity of this, we have recalculated the volume transport with more flexible widths of the subareas in Figure 6. Assume that the boundary between ADCP j and $j+1$ is moved southwards a distance Δw_j. Then $ws_j \rightarrow ws_j + \Delta w_j$ and $wn_{j+1} \rightarrow wn_{j+1} - \Delta w_j$. In order to estimate values for Δw_j that will give better fits with the altimetry, a regression analysis is made between volume transport and the MSLA-change across the section: $Q(t) = \alpha + \beta \cdot \Delta z(t)$. The values Δw_j for each week are then modified to change the ADCP-derived volume transport towards a value that fits better with the value given by the regression for that week. To retain realistic widths, the maximal change Δw_j allowed for each area is 25% of the original width (e.g., $ws_j \rightarrow 1.25 \cdot ws_j$ and $wn_{j+1} \rightarrow 0.75 \cdot wn_{j+1}$). After modification, the regression coefficients have to be recalculated and an iterative procedure was implemented involving alternate width modifications and regression analyses.

After convergence, this procedure gave a time series for ADCP-based volume transport that had a correlation coefficient of 0.87 with $\Delta z(t)$. The regression coefficient was $\beta = 0.29 \pm 0.08$ Sv·cm^{-1}. For the twenty weeks long observational period, the average volume flux after modification was 2.8 Sv. If we use the final values for the regression coefficients and the average of $\Delta z(t)$ for the whole altimetry period, we get an average volume transport of 2.3±0.3 Sv for the whole period (Oct 1992 to July 2012). Averaging over the 1995-2009 period used by Berx et al., yields 2.2±0.3 Sv. The uncertainties quoted here are purely from the statistical analysis and do not involve other sources of uncertainty.

6. Comparison between MSLA-changes across the Z-section and the S-section

The lack of overlap between ADCP coverage at the two sections means that we cannot compare transport estimates at the two sections based on the ADCP measurements, solely. Berx et al. (2013) have suggested, however, that a transport estimate based upon the MSLA-change across the S-section may give a fair representation of the variation of the Atlantic water flow through that section. We can therefore compare the ADCP-based transport through the Z-section with the MSLA-change across the S-section. For the original ADCP-based transport, the correlation coefficient was only 0.33, which increased to 0.34 when using the modified transport series.

One reason for this is seen if we correlate the MSLA-changes across the two sections with one another and, here, we can use the full altimetry data set, dating back to 1992. With weekly averages, the correlation coefficient between (s6-s0) and (z6-z2) is only 0.51. Using annual averages (52 weeks), this correlation coefficient becomes 0.42. The difference between the two MSLA-changes is illustrated in Figure 8, which also shows that a better correspondence would be obtained by extending the Z-section all the way to point z0 (red curve in Figure 8).

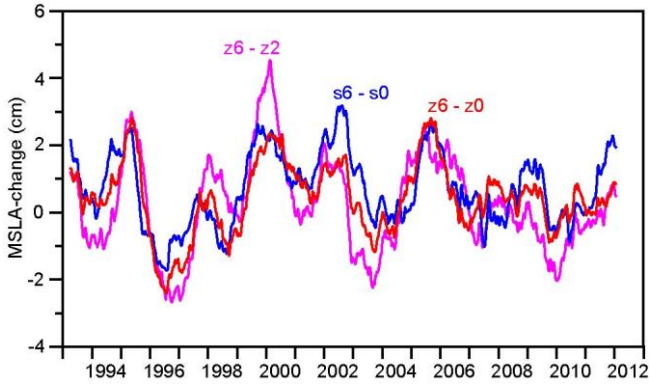

Figure 8. Annually averaged (52 week running mean) MSLA-change across the channel at the two sections. For the S-section (blue), the MSLA-change is between points s0 and s6. For the Z-section the change is shown both from point z2 to z6 (purple) and from point z0 to z6 (red).

The MSLA-change across the extended Z-section (red curve in Figure 8) fits much better with the MSLA-change across the S-section (blue curve in Figure 8), but there are still differences, indicating that there are cross-isobathic flows between z0 and s0 and between z6 and s6. As illustrated in Figure 9, these differences are considerably smaller than the MSLA-changes across the sections.

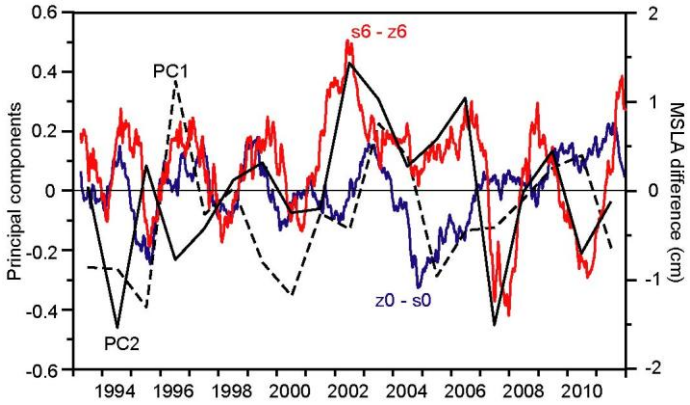

Figure 9. The difference between annually averaged (52 week running mean) MSLA values at points z0 and s0 (blue) and at points z6 and s6 (red) plotted together with the two principal components associated with modes 1 and 2 in the altimetry data for the FSC (Figure 10).

To investigate them in more detail, we have performed an EOF analysis of the altimetry data in the FSC, using annually averaged data. In order to focus on dynamical features associated with surface slopes, a time series of the spatially averaged MSLA value for the whole region analyzed was subtracted from each point before the EOF analysis. The first two modes both seem associated with recirculation in the FSC (Figure 10).

The MSLA difference between the endpoints (z0 and s0) on the Faroe side (blue curve in Figure 9) bears some resemblance to PC1, whereas PC2 seems to explain the difference in MSLA difference between points s6 and z6 fairly well (red curve in Figure 9) except for the period before 1997, when PC1 exhibited the most extreme variations.

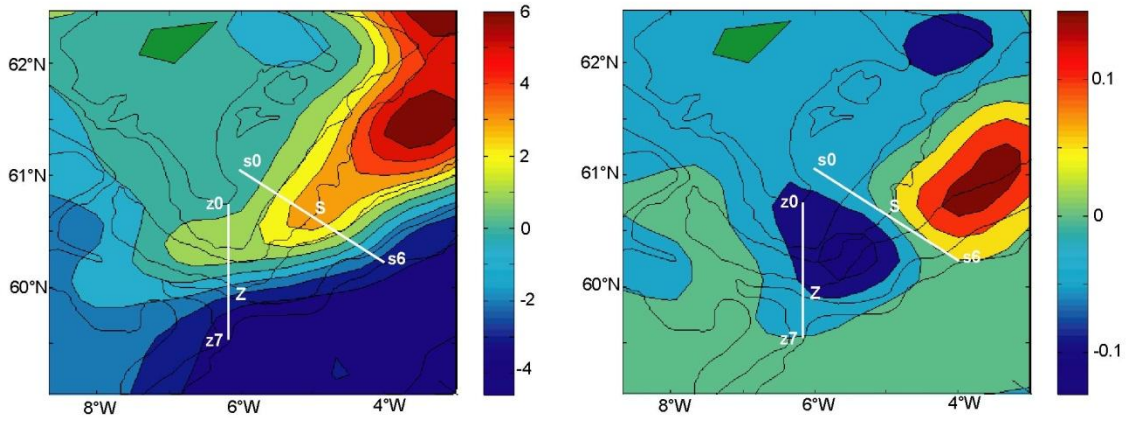

Figure 10. The first two modes of MSLA in the FSC based on the altimetry data. Before the analysis, the temporally varying spatial average has been subtracted from each point at each time. Mode 1 explains 37% of the variance and mode 2 explains 18%. The two sections are indicated by white lines with selected altimetry points indicated.

To investigate the relationship between the altimetry EOF modes and the velocity variations, we averaged velocities at the four main ADCP sites on the S-section over the uppermost 325 m and calculated annual averages. These were correlated with the principal components associated with the two modes in the annually averaged altimetry (Figure 10). The result (Table 5) shows the expected behaviour of currents with changing PC1. When there is strong recirculation, i.e. PC1 is strongly negative, along-channel velocity on the Faroe side (B) is also negative, i.e. towards the southwest, whereas currents on the Shetland side (D and E) increase towards the northeast. This situation also tends to get cross-channel velocities towards Shetland at sites B and D, whereas C and E seem less affected.

Table 5. Correlation coefficients between annual averages of the first two principal components and along-channel (Al, directed towards 38°) and cross-channel (Cr, directed towards 308°) velocities at four ADCP sites on the S-section, averaged over the uppermost 325 m. "Years" indicates number of years in the analysis. Only years with at least 11 months (335 days) of data were included for each site.

Site	Years	PC1-Al	PC2-Al	PC1-Cr	PC2-Cr
SB	7	0.82	0.39	0.47	0.74
SC	11	-0.36	0.13	-0.15	0.95
SD	8	-0.67	-0.16	0.59	0.85
SE	9	-0.39	0.35	-0.34	0.45

The cross-channel velocities on the S-section are, however, much better correlated with PC2, especially for the two central ADCP sites SC and SD. Figure 11 illustrates the correspondence between PC2 and the cross-channel velocity at SC. Normally, the cross-channel flow is negative, that is towards Shetland at this site. With high positive PC2 values, this component is reduced to zero (note that cross-channel here is defined as parallel to the section). With a strongly negative PC2, the normal cross-channel velocity at SC is enhanced, indicating stronger recirculation at this location. Thus, the good correspondence between the red curve in Figure 9 and PC2 after 1997 may be explained by cross-channel flow that crosses isobaths over the Shetland side slope of the channel.

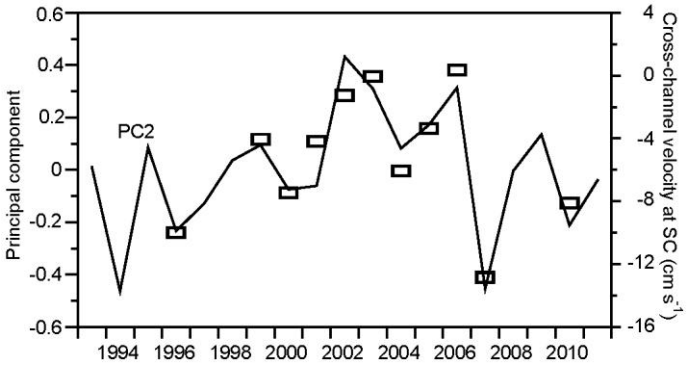

Figure 11. The second principal component (black line) and annually averaged cross-channel velocity (towards 308°) at ADCP site SC on the S-section (open rectangles).

7. Altimetry-based volume transport

The comparison between MSLA-changes across the two sections illustrates some of the problems associated with using MSLA-change to estimate volume transport. If we compare transports through two sections, continuity requires coherence. Since the thickness of the Atlantic layer between the sections may vary in time, the two transports need not be equal, but on long timescales, the difference has to be small unless there is considerable diapycnal mixing. A rough estimate of the area between the two sections at the depth of the 5°C-isotherm (10^4 km^2) and its vertical variation (100 m, see Figure 13) implies that on annual timescales, the transport difference should be less than 0.1 Sv.

According to Berx et al. (2013), the conversion factor between MSLA-change and volume transport is 0.29 Sv cm^{-1} for the S-section. For the Z-section, we found the same value (Part 5). From Figure 8, we see that the difference between (z6-z2) and (s6-s0) may exceed 2 cm, even after annual averaging, which implies a difference in volume transport of more than 0.5 Sv, clearly violating continuity. If we use the MSLA-change from z0 to z6 (red curve in Figure 8) instead of the change from z2 to z6 (purple curve in Figure 8), the difference is less, although still too high.

Table 6. Correlation coefficients between annually averaged MSLA-changes across neighbouring altimetry points on the Z-section.

	(z2-z1)	(z3-z2)	(z4-z3)	(z5-z4)	(z6-z5)	(z7-z6)	(z8-z7)	(z9-z8)
(z1-z0)	0.84	0.16	-0.76	-0.90	-0.80	-0.47	0.12	0.05
(z2-z1)		0.64	-0.43	-0.83	-0.85	-0.60	-0.04	-0.11
(z3-z2)			0.39	-0.20	-0.46	-0.55	-0.36	-0.33
(z4-z3)				0.80	0.53	0.08	-0.41	-0.31
(z5-z4)					0.92	0.54	-0.15	-0.10
(z6-z5)						0.81	0.14	0.10
(z7-z6)							0.64	0.48
(z8-z7)								0.91

This seems to imply that we have to include the region north of z2, when calculating Atlantic water transport through the Z-section. To investigate this conjecture further, we computed annual averages of MSLA-changes across each of the 9 intervals between two neighbouring altimetry points on the Z-section and then cross-correlated them. The result (Table 6) confirms that in the region north of z2, sea level tilts are correlated with the tilt over the Faroe side of the slope (z2 to z3) and anti-correlated with the tilts over the Shetland side (z3 to z7). This implies that the region from z0 to z2 is involved in the recirculation of Atlantic water through the channel and may explain why the exclusion of this region gives an MSLA-change across the Z-section (purple curve in Figure 8) that is more variable and less coherent with the change across the S-section, as compared to the MSLA-change from z0 to z6 (red curve in Figure 8).

To use MSLA values for estimating transport variations, some conditions have to be fulfilled. We assume geostrophy to be valid on timescales of a week or beyond, but geostrophy only connects sea level tilt and surface velocity. If, however, the average velocity between the surface and depth D is proportional to the surface velocity ($u_a(t) = a_0 \cdot u_s(t)$), then it is easily shown (Berx et al., 2013) that the volume transport $q(t)$ from the surface down to depth D between two altimetry points is given by the change in absolute sea level $\Delta h(t)$ between the two points:

$$q(t) = \frac{g \cdot D \cdot a_0}{f} \cdot \Delta h(t) \equiv \beta \cdot \Delta h(t) \qquad (2)$$

The total transport between altimetry points z0 and z6 can then be found as the sum:

$$Q_z(t) = \sum_{i=0}^{5} q_i(t) = \sum_{i=0}^{5} \beta_i \cdot \Delta h_i(t) = Q_0 + \sum_{i=0}^{5} \beta_i \cdot (\Delta h_i(t) - \langle \Delta h_i \rangle) \qquad (3)$$

where $q_i(t)$ is the transport between points i and $i+1$ on the Z-section, Q_0 is the average volume transport, and $\langle \Delta h_i \rangle$ the average sea level change across interval i. Without knowledge of the absolute sea level, the average transport cannot be derived from this but the variations in transport should still be given by Equation (3) with $\Delta h_i(t)$ replaced by the differences in MSLA between altimetry points. Based on Equation (3), we have generated a time series for $Q_z(t)$ using the values for $\beta_i = g \cdot D_i \cdot a_{0i} / f$ given in Table 6, where D_i is the average depth of the 5°C-isotherm or bottom in each interval and a_{0i} was assumed equal to *1* over the shallow part of the section between z0 and z2 and equal to *0.78* over the rest of the section (Table 4). For Q_0, we use the value 2.7 Sv from Berx et al. (2013).

Table 6. Values for the coefficient β_i (in Sv·cm^{-1}) in Equation (3) for each interval on the Z-section.

Altimetry interval:	z0 – z1	z1 – z2	z2 – z3	z3 – z4	z4 – z5	z5 – z6
β_i:	0.19	0.26	0.27	0.31	0.36	0.24

The resulting time series $Q_z(t)$ (red curve in Figure 12) may be compared with the time series for volume transport through the S-section published by Berx et al. (2013), which is given by:

$$Q_s(t) = Q_0 + \beta_s \cdot (s6(t) - s0(t)) \qquad (4)$$

where $\beta_s = 0.29$ Sv·cm^{-1} (blue curve in Figure 12). The correlation coefficient between the two series is only 0.84, but this may partly be due to cross-isobath flow between the two sections as discussed in Part 6. If we assume that the average volume transports of the cross-isobath flows are negligible, then their temporal variations may be estimated by:

$$q_{zsn}(t) = \beta_{zsn} \cdot (z0(t) - s0(t)) \qquad \textit{and} \qquad q_{zss}(t) = \beta_{zss} \cdot (s6(t) - z6(t)) \qquad (5)$$

where both transports are defined as positive when going from shallow water towards mid-channel. For the shallow inflow between the two northern endpoints $q_{zsn}(t)$, we assume that $\beta_{zsn} = \beta_0 = 0.19$ Sv·cm^{-1}. Between z6 and s6, there is considerably deeper water and there we use the same value for β as for the S-section: $\beta_{zss} = \beta_s = 0.29$ Sv·cm^{-1}.

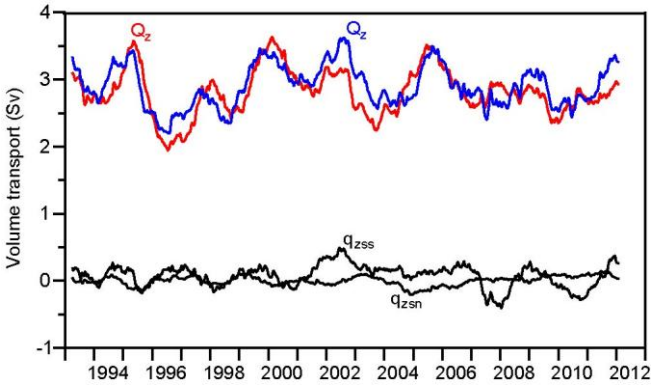

Figure 12. Annually averaged (52 week running mean) volume transports through the Z-section (red) given by Equation (3), through the S-section (blue) given by Equation (4), and cross-isobath (black) given by Equation (5).

Although the two cross-isobath transport series are considerably weaker and less variable than $Q_z(t)$ and $Q_s(t)$, they are of similar magnitudes as the difference between them. From continuity, we expect $Q_s(t)$ to be nearly equal to $Q_z(t)+q_{zsn}(t)+q_{zss}(t)$ and, indeed, the correlation coefficient between these two series is *0.96*. Instead of using Equation (4), we could have calculated $Q_s(t)$ from an equation similar to (3) with values for β_i based on Table 7 in Berx et al. (2013). That would have made no significant changes to the result.

The difference between $Q_s(t)$ and $Q_z(t)$ can therefore to a large extent be explained by the cross-isobath flows, especially $q_{zss}(t)$, which is linked to the second EOF mode of the altimetry data (Figure 10). It remains to clarify the sources of the cross-isobath flows: Do they come from the west or the east? We focus on the southern of these flows, which is stronger, and to answer the question, we correlate the MSLA-change between s6 and z6 with MSLA-changes farther south on the two sections (Table 7).

Table 7. Correlation and regression coefficients between annually averaged MSLA-changes across the interval from z6 to s6 (s6-z6) and MSLA-changes across other intervals farther south on the two sections. The analyses are based on 19 years.

	z7-z6	z8-z6	z9-z6	s7-s6	s8-s6	s9-s6
Corr. coeff.:	0.32	0.42	0.50	-0.12	0.12	0.38
Regr. coeff.:	0.18	0.38	0.64	-0.11	0.14	0.48

The correlation coefficients with the southernmost points on the S-section are low and with different signs. The southernmost points on the Z-section seem, on the other hand, to be linked to s6-z6 and a regression analysis indicates that MSLA-changes across the interval z9-z6 are more than half of the s6-z6 changes (Table 7). This indicates that at least some of the Atlantic water flowing through the deep parts of the S-section has bypassed the deep parts of the Z-section, passing south of point z6 and entering the deeper parts of the channel by crossing the isobaths between z6 and s6.

8. Atlantic layer thickness

So far, we assumed that the thickness of the Atlantic layer (bounded by the 5°C-isotherm) could be approximated as constant. From the CTD cruises along the S-section 1994 - 2009, we computed annually averaged isotherm depth at each station. Averaging these values for all the sufficiently deep stations, we find that the 5°C-isotherm varied by almost 100 m, even on inter-annual time scales (Figure 13). The variations seem to be linked to the two main EOF modes in the altimetry with maximum depth of the average 5°C-isotherm in 2002-2003, when PC2 was at its maximum.

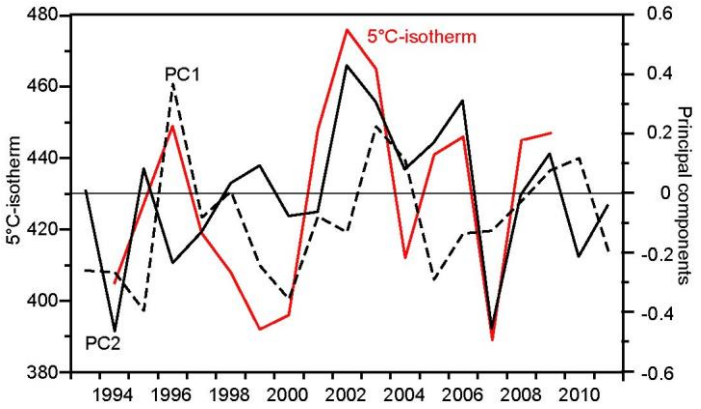

Figure 13. Annually averaged 5°C-isotherm depth (red curve) at the S-section averaged over all the sufficiently deep stations (Stations 4 – 10) and the principal components of the two main altimetry EOF modes in the FSC (Figure 10). Each value for isotherm depth is based on an average of 3 – 8 cruises in a year.

In fact, all the standard stations, except for Station 4, had their deepest 5°C-isotherm in 2002 – 2003 (Figure 14).

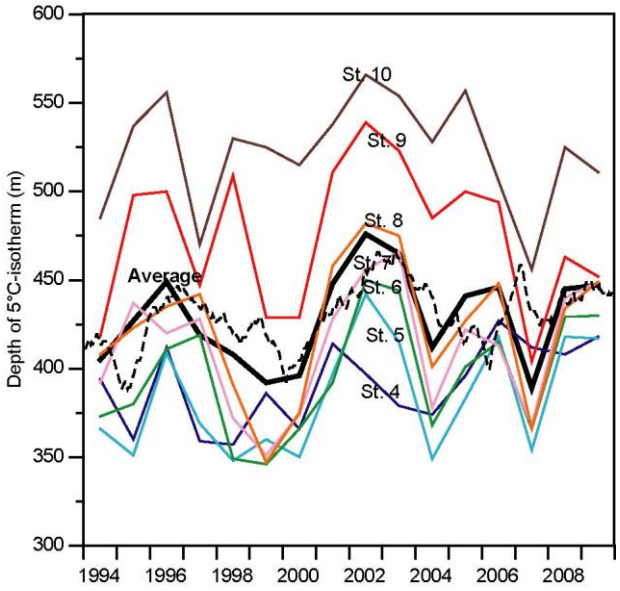

Figure 14. Annually averaged (52 week running mean) 5°C-isotherm depth at the S-section for all the sufficiently deep stations (Stations 4 – 10) and the overall average for all stations (thick black line). Each point is based on an average of 3 – 8 cruises in a year. The dashed black line shows the annually (52 weeks) averaged isotherm depth (Stations 4 – 10) generated from the regression analyses described in Part 9.

Table 8. Correlation coefficients between 5°C-isotherm depths at pairs of standard stations on the S-section. The number of data values for each correlation was between 89 and 102.

	St.5	St.6	St.7	St.8	St.9	St.10
St.4:	0.66	0.41	0.23	0.17	0.16	0.11
St.5:		0.83	0.60	0.53	0.33	0.35
St.6:			0.87	0.76	0.43	0.43
St.7:				0.93	0.64	0.57
St.8:					0.78	0.62
St.9:						0.85

This reflects the fact that 5°C-isotherm depths are positively correlated for all pairs of standard stations (Table 8), although the correlation is low between the two sides of the channel (Station 4 and Station 10). There is also a fairly high correlation (R = 0.57) between the 5°C-isotherm depth and the average sea level over the deep parts of the channel (Figure 15). If this was just a baroclinic response, we would expect the ratio between these two parameters to be equal to $\rho/\Delta\rho \approx 2000$, but a regression analysis indicates a ratio that is only around 500.

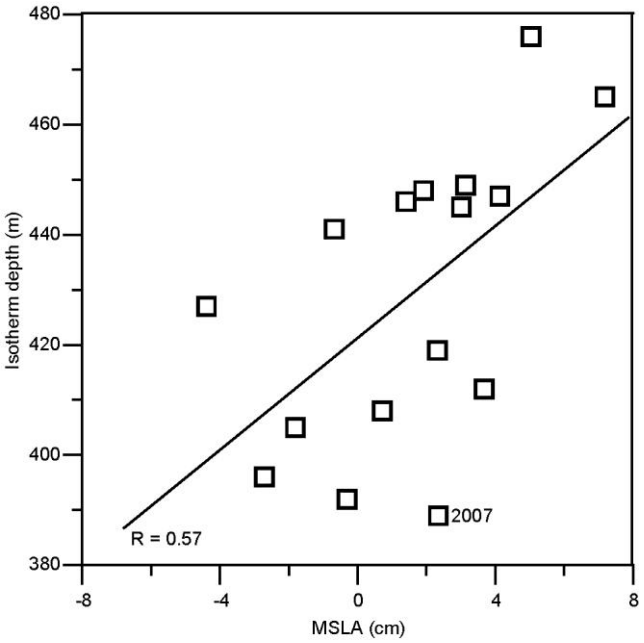

Figure 15. Annually averaged 5°C-isotherm depth at the S-section, averaged over Stations 4 to 10, plotted against annually averaged MSLA, averaged over altimetry points s2 to s5. The outlier value for 2007 is emphasized. The regression line and correlation coefficients, including 2007, are shown. If 2007 is excluded, the correlation coefficient increases to R = 0.66, and the slope of the regression line increases to 539.

Here, it must be noted that the bottom layer of the FSC is not quiescent. On the contrary, it feeds the FBC-overflow and WTR-overflow, which requires a volume transport of dense water, exceeding 2 Sv. Indeed, there seems to be a link between sea level, isotherm depth, and FBC-overflow, which co-vary, except for 2007 (Figure 16).

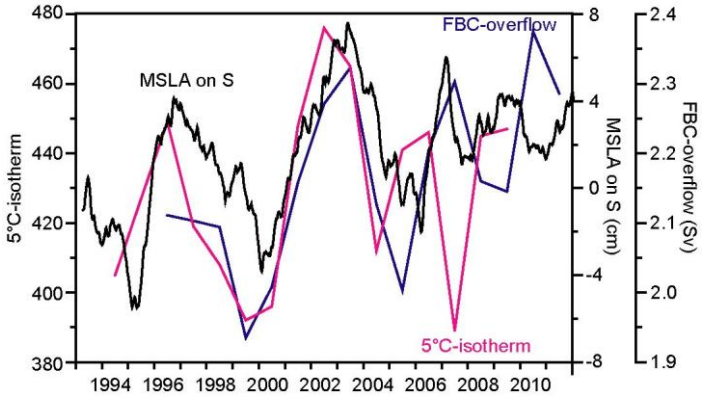

Figure 16. Annually averaged 5°C-isotherm depth at the S-section, averaged over Stations 4 to 10 (purple), MSLA on the S-section, averaged over altimetry points s2 to s5 (black), and volume transport of FBC-overflow (blue).

The link between MSLA values on the S-section and FBC-overflow would be consistent with the finding (Olsen et al., 2008) that the FBC-overflow volume transport is approximately proportional to the along-flow difference between upstream and downstream pressure at the depth of the overflow. Changing FBC-overflow may well affect the depth of the overflow layer upstream at the S-section, but the circulation of the Atlantic layer on top (Figure 10) must also be important.

9. The effects of Atlantic layer thickness variation

Whether we understand the link between MSLA variations and the 5°C-isotherm depth, or not, the existence of this link allows us to generate a continuous time series of 5°C-isotherm depth at the various standard stations. We do this by multiple regression analyses where the time series of isotherm depth at each standard station is regressed on two parameters: 1) the average MSLA value for points s2 to s5 during the same week as the cruise, and 2) the MSLA-change between a pair of altimetry points during that week, where the altimetry pair is chosen to maximize the explained variance. For the central stations (6-8), at least half the variance is explained by the regression (Table 9).

Table 9. Explained variance (R^2) of isotherm depth at individual standard stations on the S-section from multiple regression analyses on the average MSLA for altimetry points 2 to 5 and on the MSLA-change between a pair of altimetry points.

Standard station:	4	5	6	7	8	9	10
Altimetry pair:	s0-s4	s3-s4	s1-s2	s1-s2	s1-s3	s1-s4	s1-s5
Number of values:	99	102	100	101	104	100	93
Explained var. (R^2):	0.16	0.32	0.50	0.59	0.59	0.48	0.40

With the results of the regression analyses, we have simulated weekly averaged values for the 5°C-isotherm depth at each standard station for the whole altimetry period (dashed black line in Figure 14). To see the effect on volume transport of using this time-varying integration depth instead of integrating down to the fixed level of the average 5°C-isotherm depth each week, we consider the volume transport $q_D(t)$ between two neighbouring altimetry points, integrated from the surface down to depth D:

$$q_D(t) = L \cdot \int_0^D u(z,t)\, dz \qquad (6)$$

where L is the distance between the altimetry points and $u(z,t)$ is the velocity component perpendicular to the line between the points at depth z and time t. If we have an ADCP site between the two altimetry points and assume that its measured profile is representative for the whole region between the altimetry points, the integral in Equation (6) can be calculated from these profiles. For later comparison with the altimetry data, we use weekly averaged profiles and we have calculated two different versions of $q_D(t)$. The time series $q_A(t)$ is derived by integrating the ADCP measurements down to the average 5°C-isotherm depth, whereas $q_S(t)$ is derived by integrating down to the simulated 5°C-isotherm depth, which changes every week.

In the left part of Table 10, we compare the average values of these two time series, averaged for all weeks with ADCP measurements at each site. Except for site SC, which has a weak average transport, the average values for $q_S(t)$ are lower in magnitude than for $q_A(t)$ by 10-28% (column 7 in Table 10). The averages have, however, opposite signs on both sides of the channel and the differences between $q_S(t)$ and $q_A(t)$ almost cancel. Thus, we can confirm the conclusion in Berx et al. (2013) that the average volume transport is not sensitive to the assumption of a fixed 5°C-isotherm depth.

Even if this is the case, the temporal variations of the volume transport might be sensitive to this assumption. To test this, we do an analysis similar to that leading to Equation (2) in Part 7. Thus, we have assumed that the vertically averaged velocity down to depth D may be approximated by the surface velocity $u(0,t)$ times a proportionality constant a_0. Equation (6) then becomes:

$$q_D(t) = L \cdot \int_0^D u(z,t)\,dz \approx L \cdot D \cdot a_0 \cdot u(0,t) = \frac{g \cdot D \cdot a_0}{f} \cdot \Delta h(t) \qquad (7)$$

where $\Delta h(t)$ is the difference in absolute sea level between the two altimetry points and the last equality follows from the assumption of geostrophy in the surface. The absolute sea level difference is equal to its time-varying anomaly plus a constant value ($\Delta h(t) = \Delta h'(t) + \Delta h_0$) and Equation (7) can be re-written as:

$$q_D(t) \approx \frac{g \cdot D \cdot a_0}{f} \cdot (\Delta h'(t) + \Delta h_0) \equiv b \cdot \Delta h'(t) + c \qquad (8)$$

We can test this relationship for both the $q_A(t)$ and the $q_S(t)$ time series by correlating them with the MSLA-change across the interval, which represents $\Delta h'(t)$. The correlation coefficient tells us how good the relationship is, whereas a regression analysis gives us the coefficients b and c. These analyses were made on 4-week averaged data and the results are presented in Table 10.

Table 10. Comparison of volume transport between neighbouring altimetry points calculated from ADCP measurements integrated down to the average 5°C-isotherm depth $q_A(t)$ and down to the simulated 5°C-isotherm depth $q_S(t)$. The left part of the table lists average values, their difference and ratio. The right part lists correlation (R) and regression (b and c) coefficients between 4-week averaged volume transport and MSLA change according to Equation (8). The coefficient b has the unit (Sv cm^{-1}) and c has (Sv).

Altim	ADCP	Number	Average transport (Sv)				Number	q_A versus Δh			q_S versus Δh		
pair	Site	Weeks	q_A	q_S	q_S-q_A	q_S/q_A	4-weeks	R	b	c	R	b	c
s1-s2	SB	537	-0.27	-0.19	0.08	0.72	127	0.78	0.31	-0.25	0.76	0.30	-0.17
s2-s3	SY	83	-0.32	-0.24	0.08	0.75	19	0.91	0.30	0.00	0.90	0.28	0.06
s3-s4	SC	645	0.09	0.12	0.03	1.38	154	0.65	0.26	0.00	0.62	0.25	0.04
s4-s5	SG	79	0.63	0.51	-0.12	0.82	18	0.72	0.29	0.24	0.73	0.27	0.15
s4-s5	SD	621	1.85	1.66	-0.18	0.90	124	0.87	0.51	1.61	0.87	0.51	1.44

When we keep the 5°C-isotherm depth fixed at its average for each altimetry interval, the correlation coefficients (column 9 in Table 10) are similar to those reported in Table 4 of Berx et al. (2013), as expected. Our regression analysis here was not constrained to have zero offset as in Berx et al. (2013), but still the regression coefficient b (column 10 in Table 10) has similar values as the values for β in Table 7 of Berx et al. (2013), except for ADCP site SD. This site has a strong barotropic component, as seen in the value for the c coefficient (column 11 in Table 10), which may perhaps explain this discrepancy.

Remarkably, the values for the correlation coefficient (R) and the regression coefficient b are almost unchanged when we use the time-varying simulated 5°C-isotherm depth (columns 12-14 in Table 10) instead of its average (columns 9-11 in Table 10). To the extent that the use of a simulated 5°C-isotherm depth is appropriate, we therefore conclude that the assumption of a fixed 5°C-isotherm depth does not reduce the accuracy of the transport time series substantially.

Once the coefficient b has been determined for each interval between two neighbouring altimetry points, the variations of Atlantic water transport between them can be estimated for each month back to October 1992 from the altimetry data. Berx et al. (2013) used a value of 0.29 Sv cm^{-1} for the whole section between points s0 and s6 together with the average transport to generate a time series of Atlantic water transport between these two points.

This value is seen to be consistent with column 13 in Table 10, for all the ADCP sites between s1 and s5, except for site SD. The much higher value for b at site SD might tempt us to use a

strategy with different *b* values in the different altimetry intervals, but the other ADCP site in the s4-s5 interval, site SG, does not have such a high value for *b* and the *b* value for site SD is only representative for part of the s4-s5 interval. At the present level of uncertainty in the data set, the benefit of adopting such a strategy therefore seems doubtful.

10. Discussion

Compared to traditional current meter moorings, upward-looking ADCPs, deployed at depth, are less vulnerable to fisheries but they do not sample the near-surface layer. This means that ADCP profiles must be extrapolated to the surface. For the ADCP data on the Z-section, we extrapolated by assuming no shear from the uppermost bin measured (last column in Table 1) to the surface. This is probably not the best way to extrapolate and may perhaps explain the low correlation coefficients between ADCP velocity and MSLA difference for sites ZB and ZE compared to sites ZA and ZC (Table 4).

For the ADCP data on the S-section prior to the 2011-2012 experiment, used in this report, the extrapolation was made "from the vertical shear for each profile, with limiting threshold values" (Berx et al., 2013). An evaluation of this procedure may be had by considering the geostrophic profiles from the CTD data set on the S-section. Computing the geostrophic profile between a pair of standard stations with 25 m depth interval, starting at 12 m depth, we can compare the across-section velocity change over one depth interval with the one just below (Table 11). As an example, the fourth column in Table 11 lists the regression coefficient for the velocity difference from 37 to 12 m depth (Δv1) regressed on the velocity difference from 62 to 37 m depth (Δv2).

Table 11. Regression coefficients between shears at neighbouring depths. Δvn (n=1-9) is the difference in velocity between depth n·25-12 (m) and depth n·25+13 (m). "Pair" indicates the standard station pair (Figure 2b), "No" indicates the number of CTD profiles in each regression analysis. The numbers in brackets indicate 95% uncertainties of the regression coefficients.

Pair	No	Δv1/Δv2	Δv1/Δv2	Δv2/Δv3	Δv3/Δv4	Δv4/Δv5	Δv5/Δv6	Δv6/Δv7	Δv7/Δv8	Δv8/Δv9
3 4	55	0.60(.15)	0.93(.14)	0.96(.13)	0.85(.12)	0.92(.07)	0.96(.06)	0.97(.06)	0.92(.05)	0.93(.07)
4 5	99	0.39(.11)	0.86(.16)	0.96(.19)	0.82(.11)	0.89(.07)	0.92(.05)	0.92(.05)	0.91(.04)	0.88(.04)
5 6	99	0.48(.12)	0.91(.14)	1.19(.23)	0.72(.12)	0.94(.07)	1.01(.06)	0.94(.06)	0.89(.06)	0.82(.05)
6 7	98	0.56(.14)	0.59(.15)	1.00(.15)	1.01(.09)	1.03(.09)	0.92(.06)	0.91(.05)	0.91(.05)	0.89(.05)
7 8	100	0.37(.11)	0.91(.19)	1.13(.13)	0.96(.09)	0.96(.07)	0.94(.06)	0.94(.05)	0.93(.06)	0.93(.06)
8 9	99	0.31(.12)	0.87(.12)	1.13(.12)	1.04(.07)	0.96(.06)	0.90(.05)	0.94(.03)	0.92(.04)	0.90(.04)
9 10	100	0.75(.15)	0.79(.13)	0.92(.14)	0.95(.11)	0.97(.06)	0.97(.06)	0.98(.05)	0.94(.04)	0.95(.04)
10 11	79	0.52(.13)	0.82(.18)	0.93(.14)	1.03(.14)	0.98(.09)	0.95(.07)	0.90(.06)	0.89(.04)	0.90(.03)
11 12	47	0.59(.13)	0.74(.19)	1.07(.18)	1.16(.16)	1.17(.14)	1.12(.13)	1.02(.13)	0.85(.07)	0.84(.05)

The assumption of geostrophy in the surface Ekman layer is, of course, not very good but as a whole, Table 11 supports the extrapolation procedure of Berx et al. (2013) fairly well. In future studies, the procedure might be slightly optimized by using the coefficients in Table 11. It should be noted that the average volume transport calculated by Berx et al. (2013) should not be seriously affected by vertical ADCP extrapolation, since it was based on the average geostrophic velocity field, adjusted by ADCP measurements.

For the S-section, we have measurements covering a long period, whereas the Z-section was only covered completely with ADCP measurements during a few months in 2011-2012. Before drawing general conclusions based on this experiment, we therefore need to consider how representative the 2011-2012 experiment was. This is especially relevant for the period with strong westward flow through the northern part of the section in February-March 2012 (Figure 4), indicative of recirculation, since this may reduce the accuracy of transport estimates.

Associated with westward flow, geostrophy implies that sea level should be higher in the northern end of the section than in the middle. An indirect measure of recirculation may be had from

the altimetry by calculating an index *r(t) = z0(t) – z4(t)* every week *t*. In Figure 17, this index is plotted for the whole altimetry period with the period of the 2011-2012 experiment enhanced. From this figure, there is no indication that the enhanced period was special. The strong recirculation in February-March 2012, seen in Figure 4, is also clear in Figure 17, but it is not exceptional when the whole altimetry period in considered. The same conclusion is reached if we use modified recirculation indices, obtained by replacing z4 with z3 or the minimum MSLA value between z1 and z6.

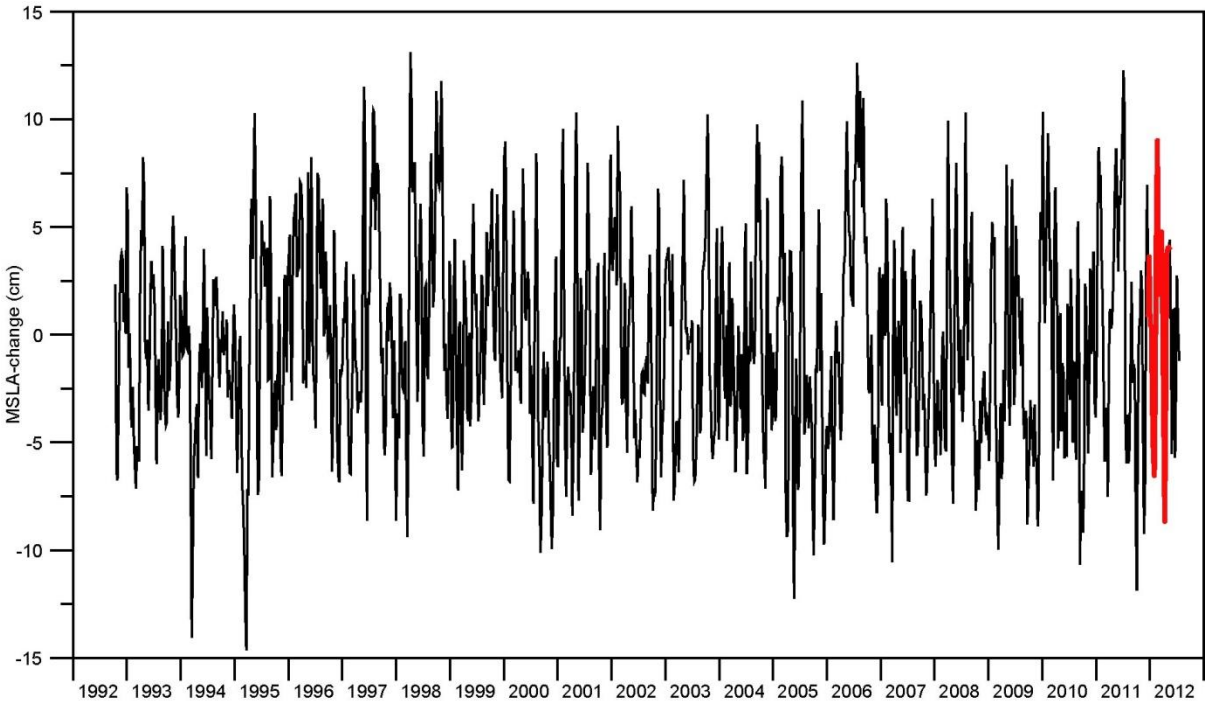

Figure 17. Weekly averaged recirculation index, defined as the MSLA-change between points z0 and z4 (*r(t) = z0(t) – z4(t)*) for the altimetry period (black curve). The thick red part of the curve is for the period 18 Dec 2011 to 10 May 2012.

11. Conclusions

Berx et al. (2013) estimated an average volume transport of Atlantic water through the FSC of 2.7±0.5 Sv for the period 1995 – 2009. Our estimate for the same period, based on the Z-section ADCPs modified by altimetry (Part 5) was 2.2±0.3 Sv. The uncertainty quoted is only from the statistical analysis and should certainly be augmented somewhat. The two results are therefore quite consistent. In response to the three questions posed at the end of the Introduction (Part 1), we furthermore find:

- As to which section is better suited for in situ monitoring, the Z-section is narrower than the S-section. With a limited number of moorings, better horizontal resolution can therefore be obtained on the Z-section. The Z-section should also be less affected by meso scale activity, but the 2011-2012 experiment clearly shows that the Atlantic water flow through this channel is not continuously uni-directional towards the Norwegian Sea (Figure 4). The strong anti-correlations between ADCPs on opposite sides of the channel (Table 3) imply substantial recirculation through the Z-section and Figure 17 indicates that this was not exceptional. We also found (Parts 6 and 7) that some of the Atlantic water, passing through the deep parts of the S-section, flows over shallow regions north or south of the deep parts of the Z-section. In situ monitoring of the Z-section therefore would require including instrumentation in these shallow regions, which are heavily fished. Finally, it should be noted that the strong overflow

current through the depths of the Z-section may lead to more excessive mooring draw-down than for deep-water moorings on the S-section, as was experienced for ZB and ZC.

- Whether temporal variations of the Atlantic water transport may be more accurately determined by in situ monitoring, or from calibrated altimetry, likely depends on the horizontal resolution of the in situ monitoring array. Through geostrophy, the MSLA-change across the section is proportional to the horizontal integral of the across-section surface velocity. Thus, it is already an integrated measure in contrast to in situ velocity measurements. For the 2011-2012 experiment, weekly averaged ADCP velocities were fairly well correlated with the MSLA-change across the altimetry interval including each ADCP site (Table 4) for most of the sites. This was the case, even after extrapolation to the surface and even though there is no guarantee that the ADCP measurements are representative for the horizontally averaged velocity over the whole interval between altimetry points. This indicates that the MSLA-changes through geostrophy can explain a large part (> 50%) of the velocity variations, not only in the surface, but throughout the Atlantic layer. The MSLA-changes therefore should explain a large part of the Atlantic water transport variations and that is confirmed for the S-section as well in Table 10. In spite of this, the most obvious integration of ADCP-velocities (Figure 6 and Equation (1)) produced a volume transport that was not impressively well correlated with the MSLA-change across the section even though the horizontal distance between the ADCPs was only on the order of the baroclinic Rossby radius (~10 km). Allowing the subareas associated with each ADCP to vary within reasonable limits did, however, lead to a relatively high correlation (Part 5). This implies that the volume transport based on ADCP data is highly sensitive to the choice of subareas associated with each ADCP. Possibly, a more refined method for horizontal interpolation of velocity between the ADCPs could improve the transport time series, but so far, the MSLA-change across the section seems to be a better indicator of Atlantic water transport variation than the ADCP-based volume transport using fixed subareas even with the high horizontal resolution on the Z-section during the 2011-2012 experiment. A similar conclusion may be drawn for the S-section from the results of Berx et al. (2013).

- The use of a fixed lower boundary for the Atlantic layer represented by the average 5°C-isotherm depth at each standard station on the S-section was found not to affect the average Atlantic water transport or its temporal variation within their uncertainties.

12. Recommendations

The long-term effort of in situ measurements in the FSC has been necessary to estimate the average Atlantic water transport and calibrate altimetry data to yield time series of its variations. The general conclusion of this study is, however, that a continuation of the in situ monitoring effort in its present form is unlikely to produce better estimates of future variations than may be had with fewer resources, as long as the altimetry measurements are maintained. This does not necessarily imply that in situ monitoring should be abandoned, but it should perhaps be re-focused and there are at least two aspects to that:

- The available estimates have been based on in situ velocity measurements that apparently have had a too coarse horizontal resolution to resolve the velocity field. One might design higher-resolution experiments to improve the calibration of altimetry data. These would

demand large resources in terms of instrumentation and would probably need to be relatively short-term and/or focused on limited parts of the section during each experiment.

- Although altimetry data may provide adequate information on the variations of the velocity field, temperature and salinity still require in situ measurements, especially sub-surface. Better data on the T/S variations are probably also necessary if the quality of existing estimates is to be improved. Available technology and fishing activity limit possible solutions, but more extensive use of autonomous gliders might be recommended. A complementary option would be deployment of relatively low-cost bottom mounted trawl-protected T/S recorders. This option is being tested for the Atlantic inflow north of the Faroes within the EU-NACLIM project and, if successful, a number of these recorders could be deployed along the slopes on both sides of the FSC to monitor the properties and vertical extent of the Atlantic layer in the channel.

Acknowledgements
The measurements during the 2011-2012 experiment were made within the THOR project (Thermo-haline Overturning – at Risk?; EU Grant Nr. 212643) and the analysis has been supported by the European Union 7th Framework Programme (FP7 2007-2013) under grant agreement n. 308299 NACLIM Project. This work has also been supported by NAACOS, which is a program funded by the Danish government.

References
Berx, B., B. Hansen, S. Østerhus, K. M. Larsen, T. Sherwin, and K. Jochumsen. 2013. Combining in situ measurements and altimetry to estimate volume, heat and salt transport variability through the Faroe–Shetland Channel, Ocean Sci., 9, 639–654.

Larsen, K.M.H., Hansen, B., Svendsen, H. (2008). Faroe Shelf Water. Continental Shelf Research 28, 1754-1768.

Olsen, S.M., Hansen, B., Quadfasel, D., Østerhus, S. (2008). Observed and modelled stability of overflow across the Greenland-Scotland ridge. Nature 455, 519-522.

P.O. Box 3051 · Nóatún 1
FO-110 Tórshavn
Faroe Islands

Tel +298 35 39 00
hav@hav.fo
www.hav.fo